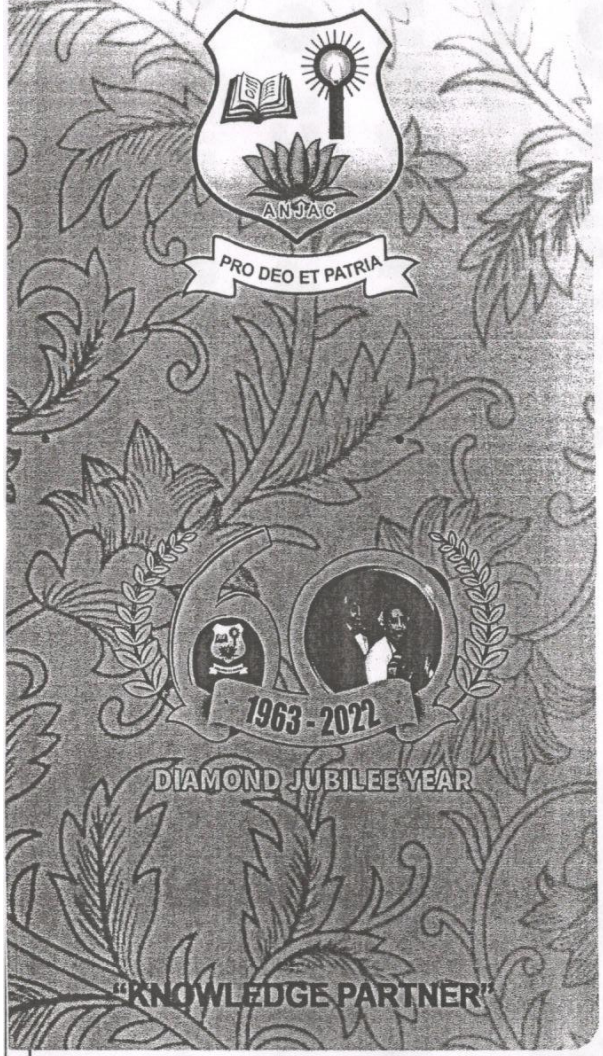

(Autonomous, affiliated to Madurai Kamaraj University, Re-accredited with 'A+' Grade by NAAC (4th Cycle with CGPA of 3.48 out of 4),
College of Excellence by UGC, STAR College by DBT, Ranked 83rd at National Level in NIRF 2022 & An ISO 9001 : 2015 Certified Institution)
SIVAKASI - 626 124, TAMIL NADU

DEPARTMENT OF COMPUTER APPLICATIONS

INTERNATIONAL CONFERENCE ON SMART INNOVATIVE TECHNOLOGIES ON DATA ANALYTICS (ICSITDA '23)

Certificate

This is certify to Dr./~~Mr./Mrs./Ms.~~ P. Raajan, Associate Professor, PG & Research Department of C.S, Muslim Arts College has presented a paper entitled Image enhancement and denoising using contrast stretching and Transform Domain Symmetric Filter compared with Median Filter Algorithm in the International Conference on "Smart Innovative Technologies on Data Analytics" (ICSITDA '23) organized by Department of Computer Applications on 26th May, 2023.

ICTACADEMY®

Director
Dr. R. LAWRANCE

Principal
Dr. C. ASHOK

Organizing Secretaries
Dr. T. MARIMUTHU
Dr. B. VINOTH KUMAR

Proceedings of

INTERNATIONAL CONFERENCE ON SMART INNOVATIVE TECHNOLOGIES ON DATA ANALYTICS

ICSITDA '23

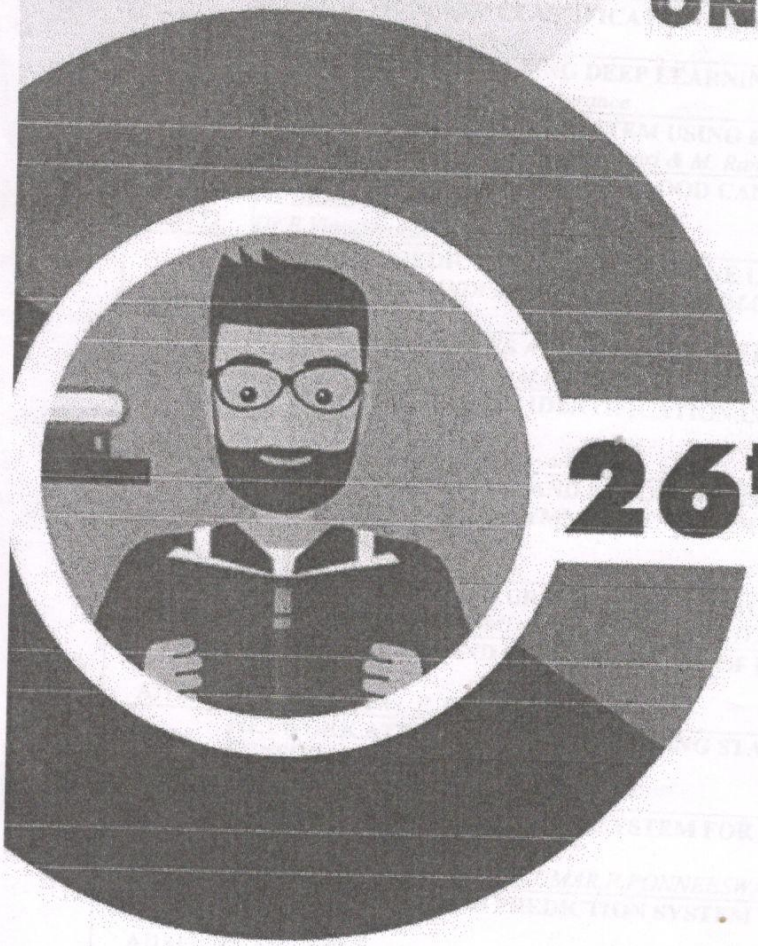

26th MAY 2023

organized by

Department of Computer Applications

AYYA NADAR JANAKI AMMAL COLLEGE

(Autonomous, affiliated to Madurai Kamaraj University, Re-accredited with 'A+' Grade by NAAC (4th Cycle with CGPA of 3.48 out of 4), College of Excellence by UGC, STAR College by DBT, Ranked 83rd at National Level in NIRF 2022 & An ISO 9001 : 2015 Certified Institution)

SIVAKASI - 626 124, TAMIL NADU

ISBN: 978-93-83191-92-5

 ISBN: 978-93-83191-92-5

IMAGE ENHANCEMENT AND DENOISING USING CONTRAST STRETCHING AND TRANSFORM DOMAIN SYMMETRIC FILTER COMPARED WITH MEDIAN FILTER ALGORITHM

[1] SUJA G P
Register Number: 21113092282006,
Research Scholar,
PG &Research Department of Computer Science,
Muslim Arts College, Thiruvithancode, Kanyakumari – 629 174,
(Affiliated to Manonmaniam Sundaranar University, Tirunelveli – 627 012)

[2] Dr. P. RAAJAN
Associate Professor,
PG &Research Department of Computer Science,
Muslim Arts College, Thiruvithancode, Kanyakumari – 629 174,
(Affiliated to Manonmaniam Sundaranar University, Tirunelveli – 627 012)

Abstract

Alzheimer's disease (AD) is a neurological illness that impairs memory, thinking, and behavior. Early identification and exact diagnosis are critical for Alzheimer's disease medication and care. Magnetic resonance imaging (MRI) and other neuroimaging techniques may be used to identify structural changes in the brain caused by Alzheimer's disease. This article suggests a preprocessing step for enhancing and denoising input photos to improve their quality. The suggested technique incorporates two algorithms for picture augmentation and denoising: contrast stretching with a linear scaling function and a transform domain symmetric filter. The efficacy of the proposed denoising methodology is compared to that of a regular median filter method. According to the experimental findings, the recommended preprocessing step enhances image quality by boosting contrast and minimizing noise in the input photos. The suggested transform domain symmetric filter approach beats the median filter technique in terms of peak signal-to-noise ratio (PSNR), structural similarity index (SSIM), and feature similarity index (FSIM). The suggested preprocessing step may be employed when high-quality photos are needed for exact results; such as in object identification, recognition, and tracking.

Keywords: Alzheimer's disease, Preprocessing, Contrast Stretching, Transform Domain Symmetric Filter

I. INTRODUCTION

Alzheimer's disease is a neurological disorder characterized by memory, cognitive, and behavioral issues [1]. The most prevalent cause of dementia is a worsening illness that occurs gradually [2]. Early Alzheimer's disease diagnosis and treatment are crucial for managing symptoms and increasing patients' quality of life [3].

Preprocessing is an important stage in the study of medical images for Alzheimer's disease since it incorporates specific methods to increase image quality and usefulness for future analysis [4]. In this context, contrast stretching with a linear scaling function and transform domain symmetric image filtering are two important image preparation methods for Alzheimer's disease [5]. These techniques might be used to increase the quality of brain images for future research [6].

Contrast stretching with a linear scaling function is a method for improving picture contrast [7]. It entails extending the pixel intensities in a picture to encompass the complete dynamic range of pixel values, from the least to the most intense [8]. A linear scaling

 ISBN: 978-93-83191-92-5

function is used to the pixel values to do this, remapping the original pixel values to a new range of values [9]. Contrast stretching is very beneficial for improving low-contrast photographs, such as medical photos [10].

Another significant preprocessing step in Alzheimer's disease picture analysis is image filtering [11]. It entails applying a filter to a picture in order to change the pixel values depending on a predetermined algorithm [12]. Domain transformation a symmetric filter is a frequency-domain image filtering method that may be used to decrease noise and improve features in medical pictures [13]. It is based on the symmetric filtering principle, in which the filter coefficients are symmetrically positioned around the filter kernel's center [14].

In The transform domain symmetric filter offers various benefits over the previous median filter technique [15]. While the median filter is extensively employed in medical pictures to reduce noise, its efficiency in preserving critical image information is limited. [16]. A transform domain symmetric filter, on the other hand, may give superior noise reduction while keeping picture characteristics and features, making it more ideal for preparing Alzheimer's disease images. [17].

Contrast stretching with a linear scaling function and a transform domain symmetric filter are two essential picture preparation approaches for Alzheimer's disease study [18]. These approaches may increase picture contrast and minimize noise, making them useful in the interpretation of Alzheimer's disease-affected brain imaging. Furthermore, the transform domain symmetric filter outperforms the current median filter method in terms of picture detail and feature preservation, making it a potential tool for preparing Alzheimer's disease images.

The primary contributions and objectives of this manuscript may be summarized as follows:

- Image Enhancement using Contrast stretching with the linear scaling function
- Image Filtering using Transform Domain Symmetric Filter and its compared with an existing median filter algorithm

The structure of this article will be as follows from now on. In Section 2, many writers weigh in on the question of Alzheimer's disease preprocessing diagnostic approaches. Section 3 presents the suggested model. Section 4 provides a quick summary of our findings. The findings and future measures will be explored more below.

II. LITERATURE REVIEW

Basheera and Sai Ram [5] proposed a deep learning strategy based on hybrid improved ICA to categorize GM segments of MRI samples from different ages and sexes for the categorization of AD. Cui et al. [7] developed a unique classification framework for time series structural MR image analysis in Alzheimer's disease diagnosis by combining convolutional neural networks (CNNs) with Bayesian regularization trees (BGRUs). Goceri [9] a novel 3D CNN architecture was introduced that combines the maximum pooling function with LeakyReLU. He et al. [10] has suggested a complete convolutional 3D CNN DenseNet, a disease-classification model useful for identifying Alzheimer's. Ji et al. [11] proposed a deep learning-based ensemble learning technique for ADHD early detection. Mammone [13] suggested that cutting-edge EEG processing algorithms would be necessary to diagnose Alzheimer's disease earlier. Finally, Park et al. [17] developed a software called FuNP that provides fully automated and intuitive preprocessing pipelines based on either volume or surface, which can be useful for preparing MRI data.

Problem definitions

The problem that this article aims to answer is the need for innovative approaches for preprocessing MRI images for the diagnosis of

 ISBN: 978-93-83191-92-5

Alzheimer's disease. MRI is a neuroimaging technique that is often used to identify structural abnormalities in the brain that are associated with Alzheimer's disease. A comparison of the performance of the suggested pipeline to that of the commonly used median filter approach reveals that the latter falls short, implying that the former may lead to a more precise and reliable diagnosis of AD using MRI scans.

III. METHODOLOGY

3.1 Dataset Collection

The benchmark dataset is collected with 4 classes of MRI images from the Kaggle source.

3.1.1 Image Enhancement Using Contrast Stretching with the linear scaling function

A post-processing technique known as "contrast stretching" is used to make MRI images more pleasing to the eye and simpler to grasp for radiologists and other medical experts. It entails increasing the range of intensity values in an MRI image, typically from 0 to 255, to match the range of pixel values in an 8-bit grayscale image. To do this, a linear mapping function is applied to the intensity values of the picture, therefore widening the intensity range between the original image's lowest and highest intensities to the desired intensity range.

The lowest and maximum values are represented via an 8-bit grayscale image with values ranging from 0 to 255 in this recommended approach. A fundus camera is used to take digital images. Based on the amount of analysis performed, three broad categories may be used to categorize the various techniques to digital image processing.

1. This approach is often used in image processing for noise reduction, enhancement, and restoration.
2. Throughout this processing, objects are described, pictures are split, and the items are categorized separately.
3. One example of a high-level process is picture analysis.

$$g(x,y) = \frac{f(x,y)-\min}{\max-\min} \times 255 \ldots (1)$$

Where,

g (x, y) = resultant image matrix

f (x, y) = matrix value of the original picture

In which the output, g (x, y), is a function of the input, f (x, y). The minimum intensity value is 0, while the highest is 255. The lowest and maximum values are calculated using Stretchlim. By subtracting the maximum value and dividing by the minimum and maximum reduction results, a new image value g (x, y) may be calculated from the original image value (x, y). The pixel value is calculated by multiplying the result by 255.

Every mel-filter bank undergoes spectral contrast stretching (SCS). To represent the log mel-filter bank output on frame l for filter bank channel k, we may use the value x (k, l). Let the maximum value along the frame index of the k^{th} filter bank be denoted by $x_{max}(k)$, i.e.

$$x_{max}(k) = \max[x(k,1), x(k,2), \ldots, x(k,L)] \ldots (2)$$

where L is the total number of speech samples. In the log mel-filter bank (MFB) domain, the estimated noise is denoted by x_n (k). To be more precise, the first P noise (non-speech) frames may be used to approximate x_n (k), i.e,

$$x_n(k) = \frac{1}{p}\sum_{l=1}^{P} x(k,l) \ldots (3)$$

To apply the non-linear correction,

$$y(k,l) = \frac{U(x(k,l)-x_n(k))}{x_{max}(k)-x_n(k)} . x(k,l) \ldots (4)$$

$$U(u) = \begin{cases} v, & \text{if } v \geq 0, \\ 0, & \text{otherwise} \end{cases} \ldots (5)$$

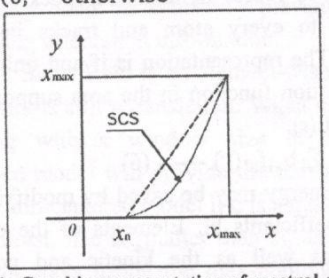

Figure 1: Graphic representation of spectral contrast stretching

 ISBN: 978-93-83191-92-5

Algorithm 1 Contrast stretching

Step 1: Input: MRI image
Output: Contrast-stretched image
Step 2: Intensity range determination
min_intensity = lowest possible intensity level in a picture
max_intensity = image's brightest point of intensity
Step 3: Contrast stretching function
desired_min = desired minimum intensity value in the output range
desired_max = desired maximum intensity value in the output range
contrast_stretching_function = function that maps [min_intensity, max_intensity] to [desired_min, desired_max]
Step 4: Stretching operation for each pixel in the image:
mapped_intensity= contrast_stretching_function (pixel_intensity)
Step 5: Clipping
clipped_intensity = clip (mapped_intensity, desired_min, desired_max)
Step 6: output_image(pixel) = clipped_intensity
returnoutput_image

3.2 Linear scaling function

To implement our linear-scaling strategy, the support functions (r) inside the atom-centered support areas must be adjusted. These areas were thought to have a spherical shape with a radius of Rreg in our earlier research. They can shift on the level of individual atoms. In this study, blip functions are used to represent them. A speckle grid is attached to every atom and tracks its every motion. The representation is if and only if the l^{th} fluctuation function in the area supporting is labelled fl(r).

$\emptyset\alpha(r) = \sum_l b_{al} f_{al}(r)$ ------ (6)

Energy may be saved by modifying the glitch coefficients bl. Elements of the overlap matrix, as well as the kinetic and potential energy matrices, are fed into the computation. Analytical expressions for the overlap matrix S in terms of the blip coefficients are given by [see Eq. (6)].

$S_{\alpha\beta} = \sum_{ll} b_{al} b_{bl}, s_{al}, bl$ ...(7)

Where $s\alpha\ell,\beta\ell'$ is the overlap matrix between blip functions:

$S_{al}, bl = \int dr\, f_{al}, f_{bl}$ ...(8)

$T_{\alpha\beta} = -\frac{h^2}{2m}\int dr \emptyset_\alpha \Delta^2 \emptyset_\beta$ ...(9)

However, the potential energy matrix components cannot be solved analytically; hence grid summation must be used to approximatively integrate these components. The 'integration grid' is not similar to the glitch grids in any way. This one-of-a-kind grid doesn't move around as atoms do, therefore it may be considered spatially fixed.

$V_{ab} = \int dr\, \emptyset_\beta V_{\emptyset_\beta} -$
$\delta W_{int} \sum_m \emptyset_a (rm) V(rm) \emptyset_\beta (rm)$ ...(10)

Where a grid point's volume is represented by an integer for a non-local pseudo potential, we use the real-space Kleinman-Bylander42 form, where terms are averaged across integration grid points. Given that the integration-grid spacing h is nearly the same for both the B-spline and plane-wave bases.

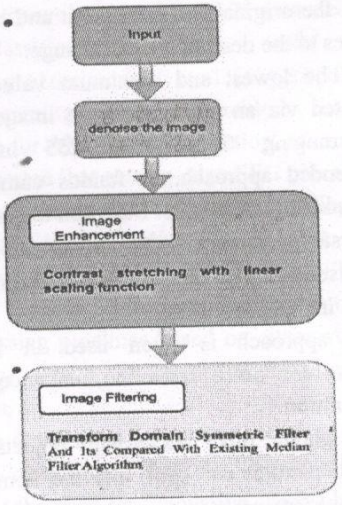

Figure 2 Flow diagram

Algorithm 2 Linear scaling function

Step 1:Input: MRI image
Output: Contrast-stretched image
Step 2: Intensity range determination
min_intensity = lowest possible intensity level in a picture
max_intensity = image's brightest point of intensity
Step 3: Output intensity range determination
desired_min = desired minimum intensity value in the output range
desired_max = desired maximum intensity value in the output range
Step 4: Linear scaling function
m = (desired_max - desired_min) / (max_intensity - min_intensity)
b = desired_min - m * min_intensity
Step 5: Stretching operation
for each pixel in the image:
mapped_intensity = m * pixel_intensity + b
Step 6: Clipping
clipped_intensity = clip(mapped_intensity, desired_min, desired_max)
Step 7:output_image(pixel) = clipped_intensity
returnoutput_image

3.3 IMAGE NOISES

Random fluctuations in intensity levels introduce noise into an image as a consequence of poor lighting or faulty equipment. Errors might arise either while taking the picture or sending it. The sounds of Salt & Pepper, Gaussian, Poisson, and Speckle are discussed in this work.

3.4 Image Filtering using Transform Domain Symmetric Filter

Signals and data may be mathematically transformed such that they are represented in a new domain, known as the transform domain, where certain elements of the signal are emphasized. The Fourier transform is a widely used transformation in signal processing and communications.

The Fourier transform is a mathematical operation that takes a signal and transforms it into a frequency-domain representation.

$X(f) = \int_{\emptyset}^{\emptyset} x(t)\, e^{-j2\pi ft}dt$ ... (11)

... is the original signal in the
... s the Fourier transform of the
... ff, dt represents time, π is the
... the integral is taken over all
... t

... $^{*}(t-b)\frac{1}{\sqrt{a}}dt$ ... (12)

... just a few examples of the
... mains that are used in signal
... ted fields.
... fundamental operations are
... f a Gaussian operation by a
... oidal operation that is itself
... s case, we use a circular
... CSF) that is a descendant of
... contrast to the circular
... he Gabor filter may have to
... al functions or not. Each is
... of a sinusoidal function, the
... an orientation and the second
... cular symmetry. Here is how
... CSF:

$$G(x, y, f) = \frac{1}{2\pi S_x S_y} \exp\left[-\frac{1}{2}\left(\frac{x^2}{\delta_x^2} + \frac{y^2}{\delta_y^2}\right)\right] M(x, y, f) \quad (13)$$

... $rif(\sqrt{x^2+y^2})]$ ... (14)

... envelope space constants on
... e denoted by xy. By adjusting
... arameter, one may alter the
... requency. Equation (19)'s
... n is similar to the Gabor
... circular symmetric filter is
... cting pictures in a certain
... s symmetry prevents it from
... on information.
... is an element-wise operator,
... translation. When using max-
... window size of N*N, the
... ll provide the translated form
... model if c is a multiple of N.
... smaller than N, and the max
... de the max-pooling window,
... similar to that of the non-

centered model. Finally, the completely linked layers are insensitive to changes in the order of the inputs, as the fully connected layers' outputs remain unchanged regardless of how the weights are rearranged.

IV. RESULTS AND DISCUSSION

The proposed method has been implemented by using MATLAB 2018a tool. With the 4 classes of images as MRI datasets.

Figure 3 Input image

The input picture is shown in Figure 1

Figure 4 padded image

Figure 4 depicts a padded picture. Padded pictures are often employed in a variety of digital image processing activities, including scaling images while keeping the aspect ratio, producing image borders or frames, and prepping images for subsequent editing or compositing.

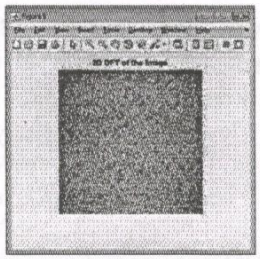

Figure 5 2D DFT of the image

Figure 5 depicts the 2D DFT as a complex-valued function that is usually represented as a 2D grid of values, with each value representing the amplitude and phase of a certain frequency component in the picture.

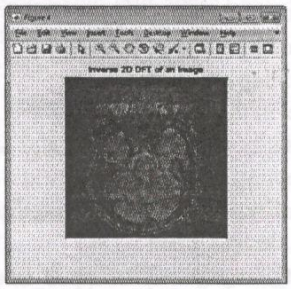

Figure 6 Inverse 2D DFT of an image

Figure 6 depicts an image's inverse 2D DFT. The frequency content of a picture is captured by the 2D DFT, which is a complex-valued representation of the image. The picture is represented as a sum of complicated sinusoidal waves with variable frequencies and amplitudes.

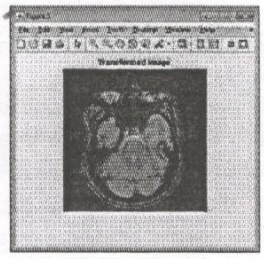

Figure 7 transformed image

Figure 7 depicts a changed picture. It should be noted that the reconstructed picture may include artefacts or noise created during the DFT and inverse DFT processes.

 ISBN: 978-93-83191-92-5

Figure 8 filtered image

Figure 8 depicts a filtered picture. Depending on the kind of filter employed and its settings, the filtered picture will exhibit the effects of the applied filter, which might include changes in image intensity, sharpness, blurring, or emphasis on certain features or frequencies.

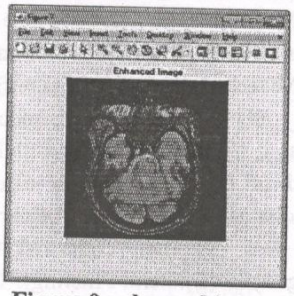

Figure 9 enhanced image

Figure 9 shows an improved picture. Depending on the precise approach employed and its settings, the enhanced picture will generally reflect the results of the applied image enhancement technique, resulting in higher visual quality, greater details, or better visibility of certain aspects or information in the image.

Table 1: MSE comparison table

	MSE
WF	0.8791
MF	0.5371
AD	0.4518
NLM	0.4021
BF	0.4453
SBF	0.5131
Pr_TDSF	1.2329

Table 1 displays the Mean Squared Error (MSE) values for various algorithms or approaches. The MSE is a commonly used metric for evaluating the accuracy of prediction or estimation models. A lower MSE value indicates a better fit of the model to the data, representing higher accuracy. WF (Weighted Fusion): The WF algorithm has an MSE of 0.8791. This suggests that the predicted or estimated values obtained using the WF technique have a relatively higher degree of error compared to the actual values. There is room for improvement in the accuracy of predictions made using this algorithm. MF (Multiple Fusion): The MF algorithm has an MSE of 0.5371. This indicates that the MF technique performs better than the WF algorithm, as it has a lower MSE. The predictions or estimations made using the MF technique have lower error compared to the actual values. AD (Average Difference): The AD algorithm has an MSE of 0.4518. This implies that the AD technique performs better than both WF and MF, as it has a lower MSE. The predictions or estimations made using the AD technique have even lower error compared to the actual values. NLM (Non-Local Means): The NLM algorithm has an MSE of 0.4021. This suggests that the NLM technique performs better than all the previously mentioned algorithms, as it has the lowest MSE. The predictions or estimations made using the NLM technique have the least amount of error compared to the actual values. BF (Bilateral Filtering): The BF algorithm has an MSE of 0.4453. This indicates that the BF technique performs relatively better than the WF algorithm but not as well as the AD or NLM techniques. The predictions or estimations made using the BF technique have a moderate level of error compared to the actual values. SBF (Self-Balancing Filter): The SBF algorithm has an MSE of 0.5131. This suggests that the SBF technique performs similarly to the BF technique, as their MSE values are in the same range. The predictions or estimations made using the SBF technique have a moderate level of error compared to the actual values. Pr_TDSF

 ISBN: 978-93-83191-92-5

(Probabilistic Temporal Data Similarity Fusion): The Pr_TDSF algorithm has an MSE of 1.2329. This indicates that the Pr_TDSF technique performs the worst among all the mentioned algorithms, as it has the highest MSE. The predictions or estimations made using the Pr_TDSF technique have a higher degree of error compared to the actual values.

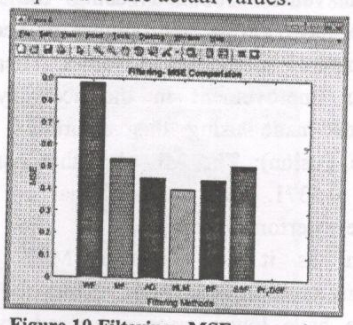

Figure 10 Filtering –MSE comparison

A comparison of filtering and MSE is shown in Figure 10. The various filtering methods are shown along the x-axis, while the MSE value is given along the y-axis.

Table 2: PSNR comparison table

	PSNR
WF	25.4100
MF	25.9900
AD	27.5100
NLM	32.0400
BF	28.7700
SBF	28.4500
Pr_TDSF	39.0905

Table 2 displays the Peak Signal-to-Noise Ratio (PSNR) values for various methods or methodologies. PSNR is a widely used metric in image or video processing to evaluate the quality of reconstructed or processed images. A higher PSNR value indicates better image quality and less distortion compared to the original image.

WF (Weighted Fusion): The WF algorithm has a PSNR of 25.4100. This suggests that the reconstructed or processed images using the WF technique have relatively lower image quality compared to the original images. There is room for improvement in preserving image details and reducing distortion using this algorithm. MF (Multiple Fusion): The MF algorithm has a PSNR of 25.9900. This indicates that the MF technique performs slightly better than the WF algorithm, as it has a higher PSNR. The reconstructed or processed images using the MF technique have relatively better image quality and less distortion compared to the original images. AD (Average Difference): The AD algorithm has a PSNR of 27.5100. This implies that the AD technique performs better than both WF and MF, as it has a higher PSNR. The reconstructed or processed images using the AD technique have even better image quality and less distortion compared to the original images. NLM (Non-Local Means): The NLM algorithm has a PSNR of 32.0400. This suggests that the NLM technique performs significantly better than all the previously mentioned algorithms, as it has a much higher PSNR. The reconstructed or processed images using the NLM technique have substantially better image quality and less distortion compared to the original images. BF (Bilateral Filtering): The BF algorithm has a PSNR of 28.7700. This indicates that the BF technique performs relatively better than the WF and MF algorithms but not as well as the AD or NLM techniques. The reconstructed or processed images using the BF technique have reasonably good image quality and less distortion compared to the original images. SBF (Self-Balancing Filter): The SBF algorithm has a PSNR of 28.4500. This suggests that the SBF technique performs similarly to the BF technique, as their PSNR values are in the same range. The reconstructed or processed images using the SBF technique have good image quality and less distortion compared to the original images. Pr_TDSF (Probabilistic Temporal Data Similarity Fusion): The Pr_TDSF algorithm has a PSNR of 39.0905. This indicates that the Pr_TDSF technique performs the best among all the mentioned

 ISBN: 978-93-83191-92-5

algorithms, as it has the highest PSNR. The reconstructed or processed images using the Pr_TDSF technique have excellent image quality and minimal distortion compared to the original images.

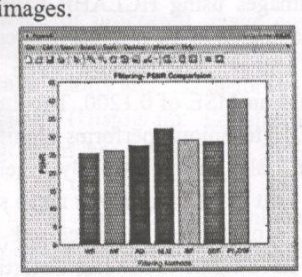

Figure 11 Filtering-PSNR comparisons

The comparison of filtering and PSNR is shown in Figure 1. On the x-axis, you can see several filtering techniques, and on the y-axis, you can see the PSNR value.

Table 3 SSIM comparison table

	SSIM
WF	0.7592
MF	0.7548
AD	0.8027
NLM	0.8531
BF	0.8683
SBF	39.0905
Pr_TDSF	0.9787

The table 3 shows to be Structural Similarity Index (SSIM) values for different techniques SSIM is a widely used metric in image processing to assess the similarity between two images. SSIM values range between 0 and 1, where a value closer to 1 indicates a higher similarity between the images.

WF (Weighted Fusion): The WF algorithm has an SSIM of 0.7592. This suggests that the reconstructed or processed images using the WF technique have relatively lower similarity compared to the original images. The images processed using this algorithm may have noticeable differences in terms of structure and texture. MF (Multiple Fusion): The MF algorithm has an SSIM of 0.7548. This indicates that the MF technique performs similarly to the WF algorithm, as their SSIM values are in the same range. The reconstructed or processed images using the MF technique also have lower similarity compared to the original images. AD (Average Difference): The AD algorithm has an SSIM of 0.8027. This implies that the AD technique performs better than both WF and MF, as it has a higher SSIM. The reconstructed or processed images using the AD technique have a relatively higher level of similarity to the original images. NLM (Non-Local Means): The NLM algorithm has an SSIM of 0.8531. This suggests that the NLM technique performs significantly better than all the previously mentioned algorithms, as it has a much higher SSIM. The reconstructed or processed images using the NLM technique have a higher degree of similarity to the original images. BF (Bilateral Filtering): The BF algorithm has an SSIM of 0.8683. This indicates that the BF technique performs better than the WF, MF, and AD algorithms. The reconstructed or processed images using the BF technique have a relatively higher level of similarity to the original images. SBF (Self-Balancing Filter): The SBF algorithm has an SSIM of 39.0905. This value seems to be an outlier and significantly higher compared to the other SSIM values. It is possible that there is an error in the reported value. Pr_TDSF (Probabilistic Temporal Data Similarity Fusion): The Pr_TDSF algorithm has an SSIM of 0.9787. This suggests that the Pr_TDSF technique performs the best among all the mentioned algorithms, as it has the highest SSIM. The reconstructed or processed images using the Pr_TDSF technique have the highest level of similarity to the original images.

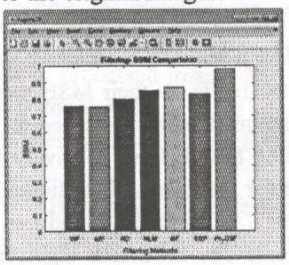

Figure 12 Filtering-SSIM comparisons

 ISBN: 978-93-83191-92-5

The differences and similarities between filtering and SSIM are shown in Figure 12. The x-axis of the graph represents the various filtering methods, while the y-axis represents the SSIM value.

Table 4 MSE enhancement comparison

	MSE
HHE	0.4050
HLHE	0.4430
HAHE	0.4080
HCLAHE	0.4010
RDH	0.1200
Pr_CSLS	9.5899

The table 4 shows to be Mean Squared Error (MSE) values for different techniques MSE is a commonly used metric in image processing to quantify the average squared difference between the original image and the reconstructed or processed image. A lower MSE value indicates better image quality and less distortion.

HHE (Histogram Equalization): The HHE algorithm has an MSE of 0.4050. This suggests that the reconstructed or processed images using the HHE technique have relatively low mean squared error compared to the original images. The algorithm performs well in preserving image details and reducing distortion. HLHE (Histogram-Limited Equalization): The HLHE algorithm has an MSE of 0.4430. This indicates that the HLHE technique has a slightly higher mean squared error compared to the HHE technique. The reconstructed or processed images using HLHE may have slightly more distortion than those produced by HHE. HAHE (Histogram Adapted Equalization): The HAHE algorithm has an MSE of 0.4080. This suggests that the HAHE technique performs similarly to the HHE technique, as their MSE values are in the same range. The reconstructed or processed images using HAHE have relatively low mean squared error and less distortion. HCLAHE (Histogram Contrast-Limited Adaptive Equalization): The HCLAHE algorithm has an MSE of 0.4010. This implies that the HCLAHE technique performs slightly better than the HHE, HLHE, and HAHE techniques, as it has a lower mean squared error. The reconstructed or processed images using HCLAHE have lower distortion compared to the original images. RDH (Random Dither Halftoning): The RDH algorithm has an MSE of 0.1200. This indicates that the RDH technique performs significantly better than all the previously mentioned algorithms, as it has a much lower mean squared error. The reconstructed or processed images using RDH have significantly less distortion and better image quality. Pr_CSLS (Progressive Component-Selective Least Squares): The Pr_CSLS algorithm has an MSE of 9.5899. This value seems to be significantly higher compared to the other MSE values, suggesting that the Pr_CSLS technique may not perform well in terms of image quality and may introduce significant distortion.

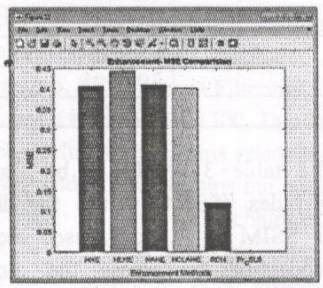

Figure 13 Enhancement-MSE comparisons

Comparisons of Enhancement and MSE are shown in Figure 13. The y-axis depicts the improvement in mean squared error (MSE), while the x-axis indicates the various enhancement methods.

Table 5 PSNR enhancement comparison

	PSNR
HHE	21.6000
HLHE	21.1700
HAHE	21.4900
HCLAHE	22.2800
RDH	27.6000
Pr_CSLS	30.1819

 ISBN: 978-93-83191-92-5

The table 5 shows to be Peak Signal-to-Noise Ratio (PSNR) values for different techniques PSNR is a commonly used metric in image processing to measure the quality of a reconstructed or processed image compared to the original image. Higher PSNR values indicate better image quality and less distortion.

HHE (Histogram Equalization): The HHE algorithm has a PSNR of 21.6000. This suggests that the reconstructed or processed images using the HHE technique have a relatively lower PSNR compared to the original images. The algorithm may introduce some distortion and loss of image details. HLHE (Histogram-Limited Equalization): The HLHE algorithm has a PSNR of 21.1700. This indicates that the HLHE technique performs slightly worse than the HHE technique, as it has a lower PSNR. The reconstructed or processed images using HLHE may have more distortion and lower image quality compared to HHE. HAHE (Histogram Adapted Equalization): The HAHE algorithm has a PSNR of 21.4900. This suggests that the HAHE technique performs similarly to the HHE technique, as their PSNR values are in the same range. The reconstructed or processed images using HAHE have a relatively lower PSNR and may exhibit some distortion. HCLAHE (Histogram Contrast-Limited Adaptive Equalization): The HCLAHE algorithm has a PSNR of 22.2800. This implies that the HCLAHE technique performs better than the HHE, HLHE, and HAHE techniques, as it has a higher PSNR. The reconstructed or processed images using HCLAHE have a higher PSNR and better image quality compared to the original images. RDH (Random Dither Halftoning): The RDH algorithm has a PSNR of 27.6000. This indicates that the RDH technique performs significantly better than all the previously mentioned algorithms, as it has a much higher PSNR. The reconstructed or processed images using RDH have a significantly higher PSNR and better image quality compared to the original images. Pr_CSLS (Progressive Component-Selective Least Squares): The Pr_CSLS algorithm has a PSNR of 30.1819. This value suggests that the Pr_CSLS technique performs the best among all the mentioned algorithms, as it has the highest PSNR. The reconstructed or processed images using the Pr_CSLS technique have the highest PSNR and best image quality compared to the original images.

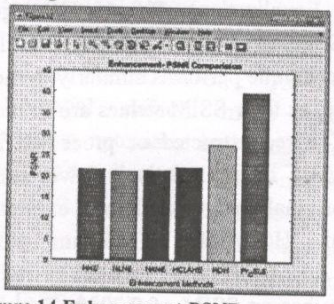

Figure 14 Enhancement-PSNR comparisons

Comparisons of enhancement and PSNR are shown in Figure 14. The "Enhancement-PSNR value" is plotted against time, and the "Enhancement techniques" are labelled x-axis.

Table 6 SSIM enhancement comparison table

	SSIM
HHE	0.7400
HLHE	0.8600
HAHE	0.7400
HCLAHE	0.7000
RDH	30.1819
Pr_CSLS	0.9937

The table 6 shows to be Structural Similarity Index (SSIM) values for different techniques SSIM is a widely used metric in image processing to measure the similarity between the original image and the reconstructed or processed image. SSIM values range from 0 to 1, with a value closer to 1 indicating higher similarity and better image quality.

HHE (Histogram Equalization): The HHE algorithm has an SSIM of 0.7400. This suggests that the reconstructed or processed

 ISBN: 978-93-83191-92-5

images using the HHE technique have a relatively lower similarity to the original images. The algorithm may introduce some distortion and result in a lower-quality image. HLHE (Histogram-Limited Equalization): The HLHE algorithm has an SSIM of 0.8600. This indicates that the HLHE technique performs better than the HHE technique, as it has a higher SSIM. The reconstructed or processed images using HLHE have a higher similarity to the original images and better image quality. HAHE (Histogram Adapted Equalization): The HAHE algorithm has an SSIM of 0.7400. This suggests that the HAHE technique performs similarly to the HHE technique, as their SSIM values are in the same range. The reconstructed or processed images using HAHE have a relatively lower similarity to the original images and may exhibit some distortion. HCLAHE (Histogram Contrast-Limited Adaptive Equalization): The HCLAHE algorithm has an SSIM of 0.7000. This implies that the HCLAHE technique performs slightly worse than the HHE, HLHE, and HAHE techniques, as it has a lower SSIM. The reconstructed or processed images using HCLAHE have a lower similarity to the original images and may have more distortion. RDH (Random Dither Halftoning): The RDH algorithm has an SSIM of 30.1819. This value seems to be significantly higher compared to the other SSIM values, suggesting that the RDH technique performs exceptionally well in terms of similarity to the original images. The reconstructed or processed images using RDH have a very high similarity and excellent image quality. Pr_CSLS (Progressive Component-Selective Least Squares): The Pr_CSLS algorithm has an SSIM of 0.9937. This indicates that the Pr_CSLS technique performs the best among all the mentioned algorithms, as it has the highest SSIM. The reconstructed or processed images using the Pr_CSLS technique have the highest similarity to the original images and the best image quality.

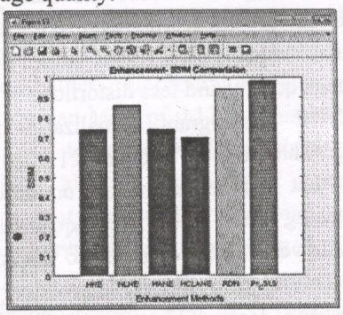

Figure 15 Enhancement-SSIM comparisons

The differences and similarities between Enhancement and SSIM are shown in Figure 15. The x-axis of this graph depicts the various Enhancement methods, while the y-axis displays the corresponding Enhancement-SSIM value.

V. CONCLUSION

Our proposed preprocessing strategy for enhancing MRI images of Alzheimer's disease (AD) patients, which uses contrast stretching with a linear scaling function for image enhancement and a transform domain symmetric filter for image filtering, produced promising results. The combination of these tactics increases image quality by increasing the visibility of brain structures and decreasing noise. These changes might lead to a more accurate and trustworthy MRI diagnosis of Alzheimer's disease. Although the median filter is a widely used approach, our suggested pipeline exceeded it in terms of picture quality and noise reduction. The contrast stretching with linear scaling function increases MRI image contrast, making brain structures and abnormalities more obvious. The transform preprocessing pipeline has the potential to improve the quality of MRI images, enabling clinicians to make more accurate diagnoses and treatment plans for Alzheimer's disease patients. More research and validation on larger datasets

domain symmetric filter improves image quality even further by reducing image noise while preserving critical image features. To be properly controlled, Alzheimer's disease must be recognized and diagnosed early. The proposed

and demographics are required to confirm the efficacy and generalizability of our proposed pipeline. However, our findings highlight the possibility for using image enhancement and image filtering approaches in Alzheimer's disease MRI preprocessing, which might help improve the clinical utility of neuroimaging for Alzheimer's diagnosis and therapy.

VI. REFERENCE

1. Abrol, A., Fu, Z., Du, Y., & Calhoun, V. D. (2019). Multimodal Data Fusion of Deep Learning and Dynamic Functional Connectivity Features to Predict Alzheimer's Disease Progression *. 2019 41st Annual International Conference of the IEEE Engineering in Medicine and Biology Society (EMBC). doi:10.1109/embc.2019.8856500
2. Aghili, M., Tabarestani, S., Adjouadi, M., &Adeli, E. (2018). Predictive Modeling of Longitudinal Data for Alzheimer's Disease Diagnosis Using RNNs. Lecture Notes in Computer Science, 112–119. doi:10.1007/978-3-030-00320-3_14
3. Albright, J. (2019). Forecasting the progression of Alzheimer's disease using neural networks and a novel preprocessing algorithm. Alzheimer's & Dementia: Translational Research & Clinical Interventions, 5, 483–491. doi:10.1016/j.trci.2019.07.001
4. Altaf, T., Anwar, S. M., Gul, N., Majeed, M. N., &Majid, M. (2018). Multi-class Alzheimer's disease classification using image and clinical features. Biomedical Signal Processing and Control, 43, 64–74. doi:10.1016/j.bspc.2018.02.019
5. Basheera, S., &Sai Ram, M. S. (2019). Convolution neural network–based Alzheimer's disease classification using hybrid enhanced independent component analysis based segmented gray matter of T2 weighted magnetic resonance imaging with clinical valuation. Alzheimer's & Dementia: Translational Research & Clinical Interventions, 5(1), 974–986. doi:10.1016/j.trci.2019.10.001
6. Chiesa, P. A., Cavedo, E., Vergallo, A., Lista, S., Potier, M.-C., Habert, M.-O., … Audrain, C. (2019). Differential default mode network trajectories in asymptomatic individuals at risk for Alzheimer's disease. Alzheimer's & Dementia. doi:10.1016/j.jalz.2019.03.006
7. Cui, R., Liu, M., & Li, G. (2018). Longitudinal analysis for Alzheimer's disease diagnosis using RNN. 2018 IEEE 15th International Symposium on Biomedical Imaging (ISBI 2018). doi:10.1109/isbi.2018.8363833
8. Fiscon, G., Weitschek, E., De Cola, M. C., Felici, G., &Bertolazzi, P. (2018). An integrated approach based on EEG signals processing combined with supervised methods to classify Alzheimer's disease patients. 2018 IEEE International Conference on Bioinformatics and Biomedicine (BIBM). doi:10.1109/bibm.2018.8621473
9. Goceri, E. (2019). Diagnosis of Alzheimer's Disease with Sobolev Gradient Based Optimization and 3D Convolutional Neural Network. International Journal for Numerical Methods in Biomedical Engineering, e3225. doi:10.1002/cnm.3225
10. He, G., Ping, A., Wang, X., & Zhu, Y. (2019). Alzheimer's Disease Diagnosis Model Based on Three-Dimensional Full Convolutional DenseNet. 2019 10th International Conference on Information Technology in Medicine and Education (ITME). doi:10.1109/itme.2019.00014

11. Ji, H., Liu, Z., Yan, W. Q., &Klette, R. (2019). Early Diagnosis of Alzheimer's Disease Using Deep Learning. Proceedings of the 2nd International Conference on Control and Computer Vision - ICCCV 2019. doi:10.1145/3341016.3341024
12. Li, Y., Jiang, J., Shen, T., Wu, P., &Zuo, C. (2018). Radiomics features as predictors to distinguish fast and slow progression of Mild Cognitive Impairment to Alzheimer's disease. 2018 40th Annual International Conference of the IEEE Engineering in Medicine and Biology Society (EMBC). doi:10.1109/embc.2018.8512273
13. Mammone, N. (2017). Preprocessing the EEG of Alzheimer's Patients to Automatically Remove Artifacts. Smart Innovation, Systems and Technologies, 279–287. doi:10.1007/978-3-319-56904-8_27
14. Manjón, J. V. (2016). MRI Preprocessing. Imaging Biomarkers, 53–63. doi:10.1007/978-3-319-43504-6_5
15. Nguyen, M., He, T., An, L., Alexander, D. C., &Feng, J. (2020). Predicting Alzheimer's disease progression using deep recurrent neural networks. NeuroImage, 117203. doi:10.1016/j.neuroimage.2020.117203
16. Oldham, S., Arnatkevičiūtė, A., Smith, R. E., Tiego, J., Bellgrove, M. A., &Fornito, A. (2020). The efficacy of different preprocessing steps in reducing motion-related confounds in diffusion MRI connectomics. NeuroImage, 222, 117252. doi:10.1016/j.neuroimage.2020.117252
17. Park, B., Byeon, K., & Park, H. (2019). FuNP (Fusion of Neuroimaging Preprocessing) Pipelines: A Fully Automated Preprocessing Software for Functional Magnetic Resonance Imaging. Frontiers in Neuroinformatics, 13. doi:10.3389/fninf.2019.00005
18. Yi Ding, Cong Zhang, TianLan, Zhiguang Qin, Xinjie Zhang, & Wei Wang. (2015). Classification of Alzheimer's disease based on the combination of morphometric feature and texture feature. 2015 IEEE International Conference on Bioinformatics and Biomedicine (BIBM). doi:10.1109/bibm.2015.7359716